Eur. Phys. J. D **12**, 27–32 (2000)

THE EUROPEAN PHYSICAL JOURNAL D

EDP Sciences

Number of electrons active in slow collisions of O^{8+} and Ar^{8+} with C_{60}

S. Martin, J. Bernard, L. Chen, A. Denis, and J. Désesquelles[a]

Laboratoire de Spectrométrie Ionique et Moléculaire[b], Université Lyon 1, Campus de la Doua, 69622 Villeurbanne Cedex, France

Received 12 November 1999 and Received in final form 28 February 2000

Abstract. Electron multiplicity has been measured for collisions of O^{8+} and Ar^{8+} with C_{60} fullerene in coincidence with the number of electrons stabilized on the projectile. Measurements have been performed at the same velocity $v = 0.24$ a.u. for both systems. The number of active electrons r is deduced from the number of stabilized electrons s and the number of ejected electrons n. The kinetic energy spectra of outgoing projectiles are different for collisions "outside" the C_{60} cage which show a narrow peak and collisions "inside" the C_{60} cage which show a broad shifted energy loss peak. The cross-sections σ_r^s for stabilization of s electrons have been measured *versus* r for each s value corresponding to peripheral collisions, *i.e.* $s = 1{-}4$ for O^{8+} and $s = 1{-}7$ for Ar^{8+}. Their sum over s, the total cross-section σ_r, shows a similar behavior for Ar^{8+} and O^{8+} up to $r = 10$. It gives a clear indication of identical multicapture processes for these two systems. The very different s number distribution is interpreted by the different relaxation modes of the multiply excited states of $O^{(8-r)+}$ and $Ar^{(8-r)+}$.

PACS. 36.40.Qv Stability and fragmentation of clusters – 34.70.+e Charge transfer

1 Introduction

During recent years, much experimental work has been devoted to the study of collisionnal properties of symmetric and stable carbon clusters. For collisions between multiply charged ions (MCI) and C_{60}, the processes investigated include multiple electron capture by the projectile and fragmentation of the fullerene molecule [1,2]. At low impact velocity ($v < 0.5$ a.u.), ionisation is very weak and multicapture is by far the dominant process. Electrons are captured in unstable multiexcited states which mainly decay *via* various cascade autoionisation processes. It is the origin of the strong electron emission observed for highly charged projectiles [3] as in ion-surface interaction [4,5]. However, some differences between MCI-C_{60} and MCI-surface collisions must be underlined. Firstly, the much shorter interaction times of the MCI-C_{60} collisions result in higher final charge states of the projectiles. Secondly, the tth ionisation potential of C_{60}, I_t, can be approximated from the energy necessary to remove the tth electron from the surface of a conducting sphere of radius R_0, $I_t = I_1 + (t-1)/R_0$, in contrast to the case of a metal surface where the work function of the conduction electrons is independent of the number of electrons removed. Finally, projectiles can be stopped in the bulk of the target in the case of interaction with a surface, whereas they only lose energy in frontal collisions with C_{60} without being stopped so that the charge state distribution can be measured. In view of these properties, a C_{60} target behaves somewhat like a "nanosurface" and its interaction with MCI can exhibit new features, especially at small impact parameters and in frontal collisions where a large number of electrons can be active in a very short time.

Several experiments have recently been performed on Ar^{8+}–C_{60} collisions. Walch *et al.* [1] have reported experimental absolute cross-sections for the stabilization of $s = 1{-}8$ electrons on argon projectiles. For 6 or 7 electrons retained by the projectile, they have observed a slight increase of the cross-section which they attributed to "inside" collisions. The stabilization of $s = 1{-}5$ electrons is related to "peripheral" collisions. In a recent paper [2], we presented the measurement of the number of ejected electrons n and the number of active electrons r *versus* the number of stabilized electrons s. Moreover, in energy gain spectra, the outgoing Ar^{2+} ($s = 6$) and Ar^{+} ($s = 7$) peaks resolve into two components due to "inside" and "outside" collisions. Stimulated by experimental results, Thumm *et al.* have developed a dynamical classical over barrier model (COBM) [6] in order to simulate the time evolution of the projectile n-shell occupation numbers. Final projectile charge states, numbers of emitted electrons and energy gain are predicted taking into account fast Auger transitions as well as rates for resonant electron capture and loss. However, this dynamical over barrier model is limited to impact parameters more or less larger than the geometrical extension of the C_{60} cage

[a] e-mail: desesque@cismsun.univ-lyon1.fr
[b] UMR 5579 du CNRS

depending on the initial projectile charge. It cannot be used for "grazing" or frontal collisions.

A similar work has been undertaken in our laboratory for the O^{8+}–C_{60} system as for Ar^{8+}–C_{60} collisions. Preliminary results obtained at 48 keV impact energy have been published as a part of a recent review paper [7]. As the oxygen velocity was significantly higher than that of argon, it was not possible to draw a final conclusion from comparison between results obtained for these two collisionnal systems. The velocity dependence of cross-sections will be presented in a forthcoming paper for Ar^{8+} and O^{8+} projectiles. In the present paper, the Ar^{8+}–C_{60} (48 keV) and O^{8+}–C_{60} (25.6 keV) collisions are studied in the same experimental conditions including the same ion velocity $v = 0.24$ a.u. and identical procedures to carefully separate inside and outside collisions. Energy gain spectra and electron multiplicity distributions of inside and outside interactions are measured for six different values of the number of stabilized electrons $s = 1-6$. Comparison of outside cross-sections with the COBM calculations and with experimental results previously obtained with the O^{8+}–C_{60} collision system shows that the primary electron transfer processes are basically the same for both systems. The strong differences observed in electron multiplicity distributions for O^{8+} compared to Ar^{8+} are tentatively explained in terms of fast relaxation of the projectiles during the interaction time.

2 Experiment

The experimental set-up has been described earlier in detail [2]. The Ar^{8+} and O^{8+} beams, produced by the electron cyclotron resonance ECR ion source of the AIM (Accélérateur d'Ions Multichargés) CEA/CNRS facility in Grenoble, are extracted at 7 kV and 3.2 kV respectively in order to accelerate them to approximately the same velocity $v \approx 0.24$ a.u. At the crossing point with a C_{60} beam, they are collimated to about 500 micrometers in diameter whereas the fullerene jet produced by an oven heated to 800 K extends to 2 mm, at about 5 mm above the 1 mm diameter oven aperture. The final charge states of the projectiles having stabilized s electrons are selected by a cylindrical electrostatic analyzer and a ceramic channel electron multiplier biased to −2.2 kV. At these high projectile velocities, the detection efficiency is approximately 100% for all charge states (from 7+ to 1+), of the outgoing projectiles. The electrons and positive ions produced are extracted on opposite sides of the collision region by a strong electric field (1 kV/cm) perpendicular to both the projectile ions and the target C_{60} beam axes as shown in Figure 1.

The charge to mass ratios of the recoil ions are determined by the time of flight (TOF) technique. A multichannel plate detector, with the first plate set to a potential of −5 kV, is used to detect charged C_{60} molecules and fragments. The relative efficiencies of detection of C_{60}^{r+} ions, measured for various voltages, are found to saturate for −5 kV. Only C_{60}^{+} and C_{60}^{2+} peaks have to be corrected for

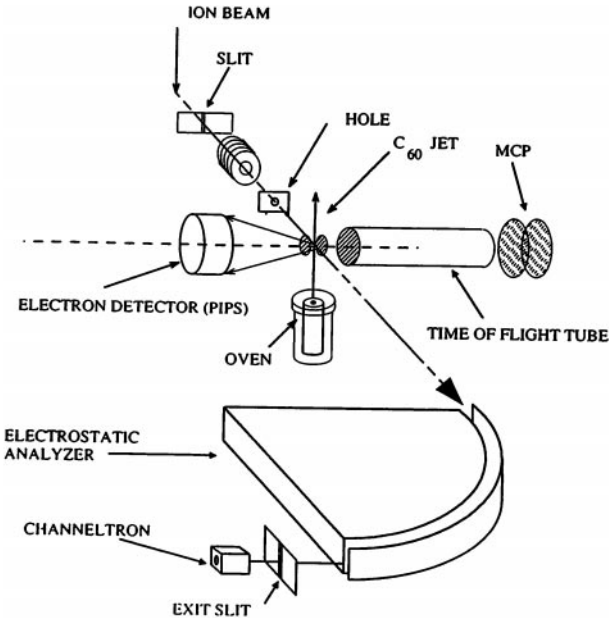

Fig. 1. Experimental set-up for measuring electron emission in coincidence with C_{60}^{r+} and charged fragments and with the final charge states of the projectiles in collision of multiply charged ions with C_{60}.

20% and 5% deficiencies respectively, as measured elsewhere [8]. The extracted electrons are sent towards a semiconductor detector (Canberra, PIPS 150-12-300) biased to 20 kV, through an intermediate focusing electrode. Trajectory simulation using the SIMION code shows that electrons with initial energy up to 300 eV are well collected and detected. The pulse height of the PIPS, proportional to the number of electrons for each event, is amplified, suitably delayed and sent to an Analog to Digital Converter (ADC 811 Ortec) *via* a Fiber Optic Transmission system (30 MHz, Math associates Inc.). The recoil ion signals are sent to a multi-hit channel of a Time to Digital Converter (TDC 3377, LeCroy). The projectile signal is delayed and used as a trigger for the conversion of the electron signal pulse and as a common stop for the TDC. The electron collection and detection efficiencies are found to be 98% for both Ar^{8+} and O^{8+} projectiles showing that their kinetic energies are indeed less than 300 eV.

3 Results

While scanning the electric field voltage applied to the cylindrical analyzer step by step, running through the outgoing oxygen beams from O^{7+} to O^{+}, the pulse height of the electron signals, the time of flight of the recoil ions and the outgoing projectile pulse are recorded in multi-coincidence. Each recorded spectrum is the sum of about 30 scans from O^{7+} to O^{+} peaks to reduce errors due to fluctuations of the O^{8+} beam intensity. Several types of two dimensional (2D) spectra are registered. The first spectra, called multistop-electron-recoil ions (EL-RI) spectra, record the electron signals and all coincident hits

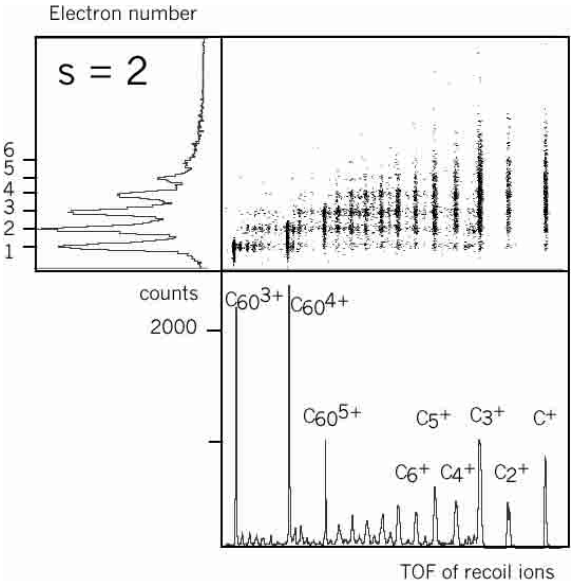

Fig. 2. Typical monostop electron-recoil ion (EL-RI) two dimensional spectrum and its X and Y projections obtained for O^{8+} + C_{60} → O^{6+}+... collisions ($s = 2$). The recoil C_{60}^{r+} are stable up to $r = 4$ with only a weak fragmentation by C_2 evaporation and fission. For $s = 5$, 6 and 7 the observed monocharged fragments are due to multifragmentation.

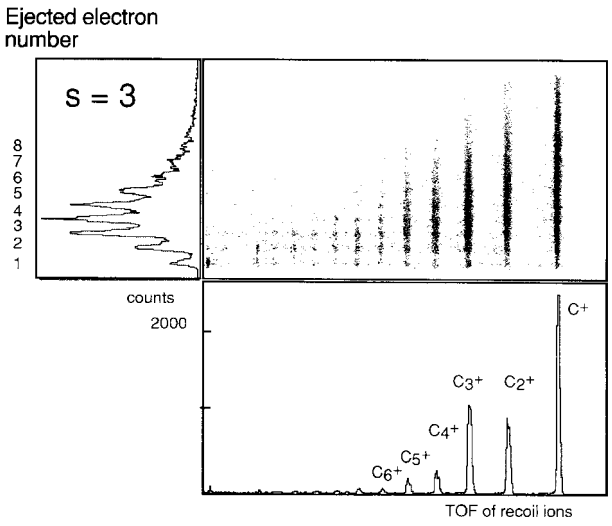

Fig. 3. Same as Figure 2, but for outgoing O^{5+} ions ($s = 3$). The distribution of the number of ejected electrons is measured up to $n = 8$ corresponding to C_{60}^{11+} primary ions which explode in small monocharged fragments.

due to recoil ions occurring in an event. In the second spectra, called monostop (EL-RI) spectra, only the hits due to the heaviest, last detected, fragments are stored. In a third kind of spectra, the electron signals and the outgoing projectiles are recorded for every event when a recoil ion is detected. They are called projectile-electron (PR-EL) spectra. They give information on the electron distributions *versus* the energy loss or gain of the projectile. Finally, in monostop projectile-recoil ion (PR-RI) spectra, the heaviest detected ion is associated with the coincident outgoing projectile. EL-RI and PR-EL spectra are the more useful ones to study the electron multiplicity distributions and the multicapture processes.

3.1 Study of electron multiplicity and break-up of C_{60}^{r+} ($3 \leq r \leq 11$) from monostop EL-RI spectra

Typical monostop EL-RI spectra are shown in Figures 2 and 3 for outgoing O^{6+} ($s = 2$) and O^{5+} ($s = 3$). The projections of the 2D spectra onto the horizontal and vertical axes give the recoil ion spectra and the distributions of the number of electrons emitted respectively. The recorded spectra have to be corrected for impurity ions located mainly between the C^+, C_2^+ and C_3^+ peaks due to the residual gas in the collision chamber as shown in Figure 2. The spots (C_{60}^{4+}, $1e$) and (C_{60}^{5+}, $2e$) are entirely due to the electron backscattering effect. The correction for this effect is performed by using the standard procedure described elsewhere [9].

For $s = 2$, the electron spectrum is mainly contributed by the intense spots (C_{60}^{3+}, $1e$), (C_{60}^{4+}, $2e$), and (C_{60}^{5+}, $3e$) corresponding to ($r = 3$, $n = 1$, $s = 2$), ($r = 4$, $n = 2$, $s = 2$) and ($r = 5$, $n = 3$, $s = 2$) respectively. The peak intensity of each electron multiplicity n is associated with the primary population of $C_{60}^{(n+2)+}$ ions. The distribution extends from 1 electron to 6 electrons corresponding to C_{60}^{3+}–C_{60}^{8+} ions. The break-up mechanisms of a given $C_{60}^{(n+2)+}$ ion can be studied from the partial horizontal projection of the 2D spectra corresponding to a selected number of emitted electrons n. Evaporation of C_2 units and asymmetric fission giving light C_2^+ and C_4^+ fragments are the main processes observed for primary C_{60}^{3+} and C_{60}^{4+} in O^{8+}–C_{60} as in Ar^{8+}–C_{60} collisions [2]. Multifragmentation is dominant for C_{60}^{5+}–C_{60}^{8+} as shown by the observation of many C_m^+ (m=1–14) and low intensity $C_{m'}^{2+}$ ($m' = 11-21$) fragments. For increasing fullerene charge states, the relative intensity of very light fragments C_m^+ ($m = 1-4$) increases. It suggests that highly charged C_{60} as C_{60}^{7+} and C_{60}^{8+} are produced in collisions where a large excitation energy is transferred to the fullerene molecules leading to their vaporization in several mono-charged light fragments. The number of electrons ejected for $s = 2$ is found larger in O^{8+}–C_{60} ($n = 1-6$; $\langle n \rangle = 2.5$) than in Ar^{8+}–C_{60} ($n = 1-4$; $\langle n \rangle = 1.8$) collisions. To explain this difference, while assuming that the multiexcited states are identically populated in both collision systems, one can consider the difference between the autoionisation cascade schemes. Indeed, the final levels of the two electrons remaining bound to the projectile are $n = 3$ for Ar^{8+} and $n = 1$ for O^{8+} which gives a greater number of autoionisation cascade channels in the case of O^{8+} than in the case of Ar^{8+}.

For $s = 3$, the electron multiplicity extends from $n = 1$ to $n = 8$ corresponding to primary populated $C_{60}^{(3+n)+}$ ions from C_{60}^{4+} to C_{60}^{11+} (Fig. 3). The mean value of the electron multiplicity is found to be $\langle n \rangle = 4$, much larger than the

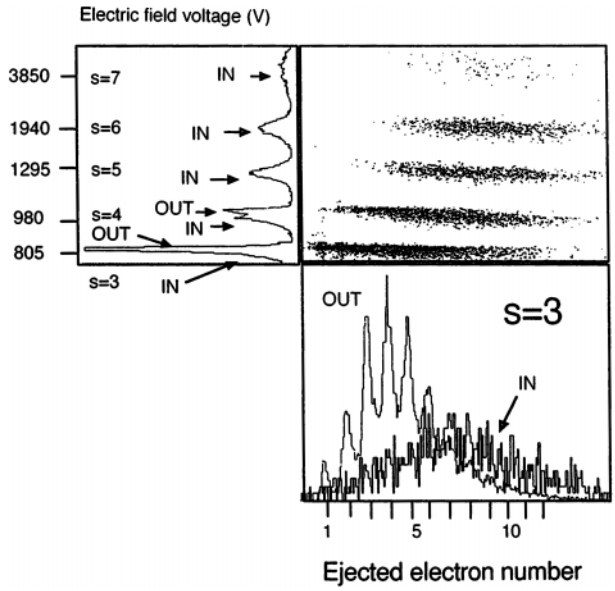

Fig. 4. Projectile-electron (PR-EL) two dimensional spectrum and its projections. The electron emission is measured in coincidence with the projectile final kinetic energy for $s = 3$, 4, ...7. The peaks IN and OUT are associated with frontal (inside C_{60} cage) and peripheral (outside C_{60}) collisions.

value $\langle n \rangle = 2$ found for Ar^{8+}. The above argument based on the number of autoionisation cascades can be asserted to explain this difference. Recoil ions detected are mainly very light monocharged fragments (C^+–C_{60}^+) which result from the multifragmentation of $C_{60}^{(4\,\mathrm{to}\,11)+}$ ions. Partial recoil ion spectra related to individual C_{60}^{r+} ions are shifted towards lighter fragments for $s = 3$ compared to the spectra obtained for $s = 2$. This result shows that the number of electrons stabilized on the projectile depends on the excitation energy of the C_{60}^{r+} ion.

3.2 Peripheral and frontal collisions from PR-EL spectra

PR-EL spectra are recorded for a number of stabilized electrons varying from $s = 1$ to $s = 7$, *i.e.* for outgoing O^{7+}, O^{6+}, ...O^+ projectiles. The part of a typical 2D spectrum shown in Figure 4 covers the $s = 3{-}7$ range. All the proceeding results are deduced from such 2D spectra.

3.2.1 Energy loss

The projection onto the vertical axis of PR-EL spectra gives the kinetic energy distribution of outgoing $O^{(8-s)+}$ ions. For $s = 3$ and $s = 4$, the signals resolve into two components labeled IN and OUT in Figure 4, attributed to frontal and peripheral collisions respectively. The contributions of peaks IN and OUT have been obtained from the unresolved energy distributions by assuming that both peaks have the same Gaussian shape but different widths. The IN-component is found to amount to 22% (75%) for $s = 3$ ($s = 4$). The peaks observed for $s = 5$, 6 and 7 are entirely attributed to IN components. The kinetic energy loss is found to be 390 ± 50 eV for O^{4+} ions following frontal collisions ($s = 4$). These values are quite close to the energy loss of such ions in a carbon foil extrapolated to an equivalent thickness (≈ 250 eV).

3.2.2 Number of electrons ejected and electron multiplicity distributions

The distributions of the number of electrons ejected are given by the projections onto the horizontal axis of the density plot. The partial projection of Figure 4 shows IN- and OUT-components separately for $s = 3$. The difference between frontal and peripheral collisions, as for the electron multiplicity, appears clearly. The mean number of electrons ejected is $\langle n \rangle \approx 8$ for peaks IN and $\langle n \rangle \approx 4$ for peaks OUT.

However, these apparent distributions have to be corrected for recoil ion efficiencies which depend on the products detected for each event. The collection and detection efficiency has been measured to be 40% for light monocharged ions (C^+–C_{10}^+) by comparing monostop and multistop spectra for $s = 2$. In fact, the probability of detecting at least one fragment in a collisionnal event depends essentially on the total number of fragments emitted. For $s = 5$, 6 and 7, fullerenes break up into many very light monocharged fragments so that detection efficiency is about 100% whereas it is approximately 0.93, 0.87 and 0.75 for $s = 4$, 3 and 2 respectively. Details of the determination of the detection efficiencies will be given in a forthcoming paper. The s dependence of the mean number of electrons ejected $\langle n \rangle$ is shown in Figure 5. It is given for frontal and peripheral collisions of O^{8+} and Ar^{8+} with C_{60}. In both collisionnal systems, a large difference in $\langle n \rangle$ values is observed between IN and OUT collisions as shown by results obtained for $s = 3$ and $s = 4$ in O^{8+}–C_{60} and for $s = 6$ and $s = 7$ in Ar^{8+}–C_{60}. For peripheral collisions with $s = 3$ and 4, the mean number of electrons $\langle n \rangle$ is about twice and three times as high in the case of O^{8+} respectively as for the case of equicharged Ar^{8+}. On the other hand, the maximum value of s for the OUT-contribution is 4 for O^{8+} and up to 7 for Ar^{8+}. In general, for the same active electron number, more electrons are ejected in the case of O^{8+} showing the important role played by the ionic core in the relaxation process. These observations are tentatively explained by the direct capture of electrons into the low lying states $n = 4$ and $n = 3$ in collisions where the number of active electrons is large. Electrons in such levels are very stable for Ar^{8+} ions but not for O^{8+}. Finally, it is remarkable that the maximum value for the sum, $\langle n \rangle + s$, is 10 for O^{8+} and 9 for Ar^{8+} which shows that the maximum number of active electrons is approximately the same in both collisionnal systems.

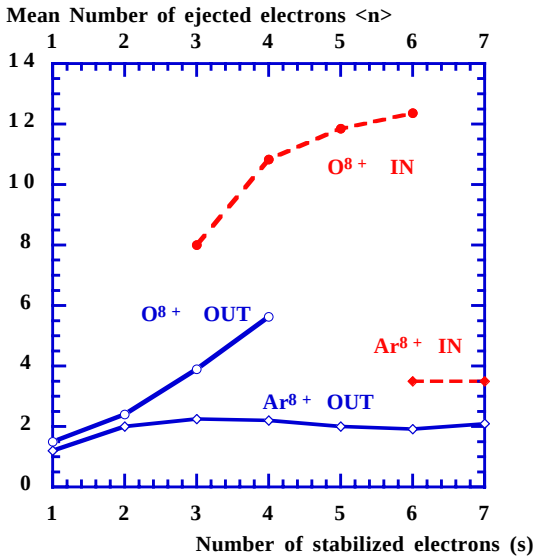

Fig. 5. Mean number of electrons ejected $\langle n \rangle$ *versus* number of electrons stabilized for (○) outside and (●) inside O^{8+} + C_{60} collisions and (◊) outside and (♦) inside Ar^{8+}–C_{60} collisions. The large differences observed between Ar^{8+} and O^{8+} are explained by the very different relaxation schemes of the multiexcited states of oxygen and argon.

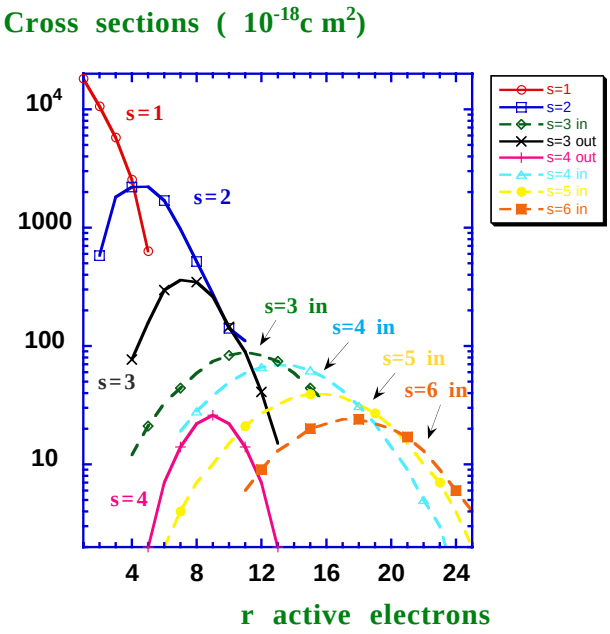

Fig. 6. Electron capture cross-sections *versus* number of active electrons for peripheral ($s = 1$–4) and frontal ($s = 3$–6) collisions between O^{8+} and C_{60}.

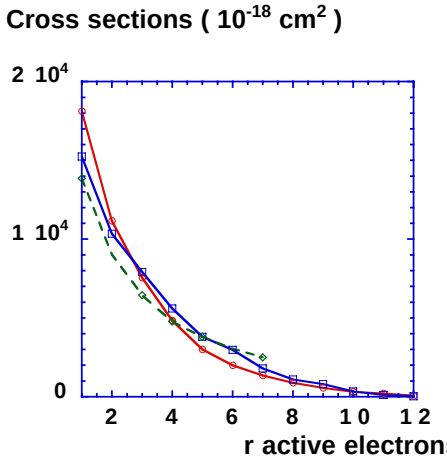

Fig. 7. Total electron capture cross-sections $\sigma_r = \sum_s \sigma_r^s$ *versus* number of active electrons for peripheral collisions. Results for (○) Ar^{8+} and (□) O^{8+} projectiles colliding on C_{60} are compared with (◊) theoretical data from CBM calculations for $s = 1$–6. The identical behaviour of Ar^{8+} and O^{8+} curves shows that the initial multielectron transfer depends only on the projectile charge state.

3.2.3 Electron capture cross-sections

The relative cross-sections σ_r^s for O^{8+}–C_{60} collisions with r active and s stabilized electrons are obtained from PR-EL spectrum projections after correction for detection efficiencies given in Section 3.2.2 above. Absolute cross-sections are deduced from the corrected values by equating the experimental total cross-section with the theoretical one $\sigma_t = 5.2 \times 10^{-14}$ cm^2 calculated using the classical over barrier model (CBM) [11] and the first ionisation potential $I_1 = 7.6$ eV for C_{60}. Results are presented in Figure 6, where IN- and OUT-components are separated when they are both present ($s = 3$ and 4). Error bars are estimated at about 20%. They are mainly due to uncertainties of detection efficiencies and to incident ion beam current fluctuations. The total frontal collision cross-section is obtained by summing the measured values 0.07, 0.07, 0.04 and 0.02 $\times 10^{-14}$ cm^2 for IN-components contributed by $s = 3$, 4, 5 and 6 respectively. It amounts to 0.2 $\times 10^{-14}$ cm^2 which is about 4% of the total cross-section. It is lower than the 0.35 $\times 10^{-14}$ cm^2 value measured in Ar^{8+}–C_{60} collisions [2]. This lower cross-section may be due to the difference in size of the electronic cores of O^{8+} and Ar^{8+}. The measured cross-sections for IN-collisions are slightly lower than the geometrical cross-section of the C_{60} cage which is 0.4 $\times 10^{-14}$ cm^2.

The total cross-sections $\sigma_r = \sum_s \sigma_r^s$ are presented as a function of the active electron number r in Figure 7 for the OUT-components. They are compared to CBM calculated cross-sections using a screening constant of 0.4 and ionisation potentials $I_r(\text{eV}) = 7.6 + 3(r-1)$ for C_{60} as in reference [12]. Only results for $r \leq 6$ are given in Figure 7 because the model can not be used for close collisions where the number of active electrons is large.

Theoretical and experimental cross-sections for electron emission present the same r dependence at large internuclear distances for both Ar^{8+} and O^{8+} projectiles. It shows that the physical picture of electrons being successively transferred from the target to the projectile given by CBM effectively describes the electron capture processes in both collision systems and that the primary multielectron transfer process depends only on the projectile initial

charge state. It confirms that the main difference between O^{8+}–C_{60} and Ar^{8+}–C_{60} collisions comes from the electron relaxation processes. In the case of O^{8+}, autoionisation is dominant and less electrons are stabilized. The numbers of active electrons can be higher than the initial charge state of the projectiles ($r > 8$ for O^{8+} and Ar^{8+}) even for peripheral collisions. Such high electron multiplicities may qualitatively be explained by electron emission during the interaction time in close collisions. Its cross-section, obtained by summing contributions of $r = 8-12$, is approximately 1% and 1.2% of the total cross-sections for Ar^{8+} and O^{8+} respectively. The corresponding internuclear distance is about 10 a.u. Thus, it concerns very close collisions, at about 0.5 a.u. from the C_{60} cage which has a radius R_0 of 9.5 a.u.

4 Summary and conclusions

Fragmentation of C_{60}^{r+} and multielectron capture processes have been studied for O^{8+} and Ar^{8+}–C_{60} collisions using coincidence measurements between ejected electrons and recoil ions, and between electrons and projectiles. Main results are provided for the multiplicity distributions of active electrons as a function of the number of electrons stabilized on the projectile. For Ar^{8+}, the stabilization of up to $s = 7$ electrons is correlated with the ejection of two electrons on average. For O^{8+}, a lower number of electrons are stabilized, $s \leq 4$ and a larger number of them, up to $\langle n \rangle = 6$, are ejected. Cross-section measurements show that the primary multielectron transfer processes are nearly identical for O^{8+} and Ar^{8+}. The projectile final charge states depend only on the relaxation schemes which are different in Ar^{8+} and O^{8+}. In peripheral collisions, the relaxation processes start after the interaction time. Only a small part, about 1%, corresponding to very close collisions, 0.5 a.u. from the C_{60} cage, can emit electrons during the interaction time. In frontal collisions, the number of electrons ejected is higher for O^{8+} than for Ar^{8+}, whereas the energy loss is nearly the same for both projectiles. The frontal collision results can be explained by a fast relaxation *via* Auger electrons which is much faster than in very close peripheral collisions, because the number of active electrons is much larger.

The authors wish to thank the SI2A staff at DRFMC/CEA Grenoble for their hospitality and help in the use of the AIM CEA/CNRS facility. This work was supported by the Région Rhône-Alpes under grant No. 97027-223 and -283, Convention Recherche, Programme Émergence.

References

1. B. Walch, C.L. Cocke, R. Voelpel, E. Salzborn, Phys. Rev. Lett. **72**, 1439 (1994).
2. S. Martin, J. Bernard, L. Chen, A. Denis, J. Désesquelles, Eur. Phys. J. D **4**, 1 (1998); S. Martin, L. Chen, A. Denis, J. Désesquelles, Phys. Rev. A **57**, 4518 (1998).
3. S. Martin, J. Bernard, L. Chen, A. Denis, J. Désesquelles, Phys. Rev. A **59**, R1734 (1999).
4. H. Kurz, F. Aumayr, H.P. Winter, D. Schneider, M.A. Brière, J.W. Mc Donald, Phys. Rev. A **49**, 4693 (1994).
5. C. Lemell, J. Stöckl, J. Burgdörfer, G. Betz, H.P. Winter, F. Aumayr, Phys. Rev. Lett. **81**, 1965 (1998).
6. U. Thumm, T. Bastug, B. Fricke, Phys. Rev. A **52**, 2955 (1995); U. Thumm, J. Phys. B **27**, 3515 (1994).
7. L. Chen, J. Bernard, A. Denis, S. Martin, J. Désesquelles, Phys. Scripta T **80A**, 52 (1999).
8. T. Schlathölter, R. Hoekstra, R. Morgenstern, J. Phys. B **31**, 1321 (1998).
9. F. Aumayr, G. Lakits, H. Winter, Appl. Surf. Sci. **47**, 139 (1991).
10. T. Schenkel, M.A. Brire, A.V. Barnes, A.V. Hamza, K. Bethge, H. Schmidt-Böcking, D.H. Schneider, Phys. Rev. Lett. **79**, 2030 (1997).
11. A. Niehaus, J. Phys. B **19**, 2925 (1986).
12. C. Yannouleas, U. Landman, Chem. Phys. Lett. **217**, 175 (1994).